International Journal of Nanomedicine

Dovepress
Taylor & Francis Group

Open Access Full Text Article

ORIGINAL RESEARCH

Multifunctional Nanozyme PDA-Cr_2O_3 for the Treatment of Osteoarthritis

Can Li[1,*], Guiju Chen[1,*], Xiongwei Yan[2,*], Bingyang Hu[3,*], Xiangyun Zhang[4], Jun Song[2,5]

[1]Department of Pharmacy, Xiangyang Central Hospital, Affiliated Hospital of Hubei University of Arts and Science, Xiangyang, Hubei, People's Republic of China; [2]Department of Orthopedics, Xiangyang Central Hospital, Affiliated Hospital of Hubei University of Arts and Science, Xiangyang, Hubei, People's Republic of China; [3]Department of Emergency Medicine, Xiangyang Central Hospital, Affiliated Hospital of Hubei University of Arts and Science, Xiangyang, Hubei, People's Republic of China; [4]Central Sterilization Supply Department, Xiangyang Central Hospital, Affiliated Hospital of Hubei University of Arts and Science, Xiangyang, Hubei, People's Republic of China; [5]Hospital Administration Office, Xiangyang Central Hospital, Affiliated Hospital of Hubei University of Arts and Science, Xiangyang, Hubei, People's Republic of China

*These authors contributed equally to this work

Correspondence: Jun Song; Xiangyun Zhang, Email doctorsj2024@163.com; wangbangjun126@126.com

Introduction: Osteoarthritis (OA) is one of the major menaces to human health. Currently, no sufficiently effective medications are available to treat OA clinically. OA is an inflammatory joint disorder. The overproduction of reactive oxygen species (ROS) plays a critical role in initiating and developing OA pathogenesis. ROS scavenging has become a vital target for OA therapy. Although chromium sesquioxide (Cr_2O_3) nanoparticle has been proven to have excellent ROS scavenging ability, its clinical application is limited due to its poor biocompatibility. Polydopamine (PDA) is an excellent carrier with outstanding biocompatibility. PDA-based nanomaterials exhibit significant potential for various ROS-related diseases.

Methods: PDA was synthesized through oxidative autopolymerization of dopamine in an alkaline environment. Subsequently, the novel nanozyme PDA-Cr_2O_3 was synthesized by loading Cr_2O_3 onto PDA nanoparticles with the assistance of hydrazine hydrate. Afterward, the cytotoxicity and ROS scavenging capacity of PDA-Cr_2O_3 were examined. Finally, the ability of PDA-Cr_2O_3 to treat OA was explored at both cellular and animal levels.

Results: PDA-Cr_2O_3 had low cytotoxicity and toxic side effects in vivo. Moreover, PDA-Cr_2O_3 exhibited a remarkable capacity to scavenge ROS both in cell-free in vitro systems, such as kit-based assays, and in cellular models. It also dramatically decreased the transcriptional level of inflammation-associated genes and the secretion of inflammatory factors of the OA chondrocytes. In animal experiments, PDA-Cr_2O_3 markedly suppressed the progression of OA.

Conclusion: PDA-Cr_2O_3 nanozyme had good biocompatibility and could effectively suppress the development of OA by efficiently scavenging ROS, which has important application prospects in OA treatment. This study might offer some new ideas for the treatment of ROS-related diseases.

Keywords: osteoarthritis, reactive oxygen species, polydopamine, chromium sesquioxide, nanozyme

Introduction

OA is the most common joint disorder worldwide, impacting about 18% of women and 10% of men over the age of 60 globally.[1] Currently, it is commonly acknowledged that OA is an inflammation-driven degenerative disorder.[2] OA is the result of a composite of risk factors, of which advanced age and obesity are the most crucial.[3] Currently, besides total joint replacement, no effective interventions exist to retard the development of OA. However, joint replacement is expensive, and artificial joints have lifetime limits.[4] The commonly used non-steroidal anti-inflammatory drugs can merely offer symptomatic relief for OA. So far, there is no specific medication that can cure OA. It is of great urgency to develop new drugs that can delay the evolution of OA. To achieve this goal, a profound understanding of the pathogenesis of osteoarthritis is needed.

Recently, accumulating evidence indicated that excessive ROS bears a close relationship to the onset and development of OA.[5] Among the ROS, the main constituents are hydrogen peroxide (H_2O_2), superoxide anions ($O_2^{\bullet-}$), and

Received: 4 May 2025
Accepted: 17 August 2025
Published: 27 August 2025

Graphical Abstract

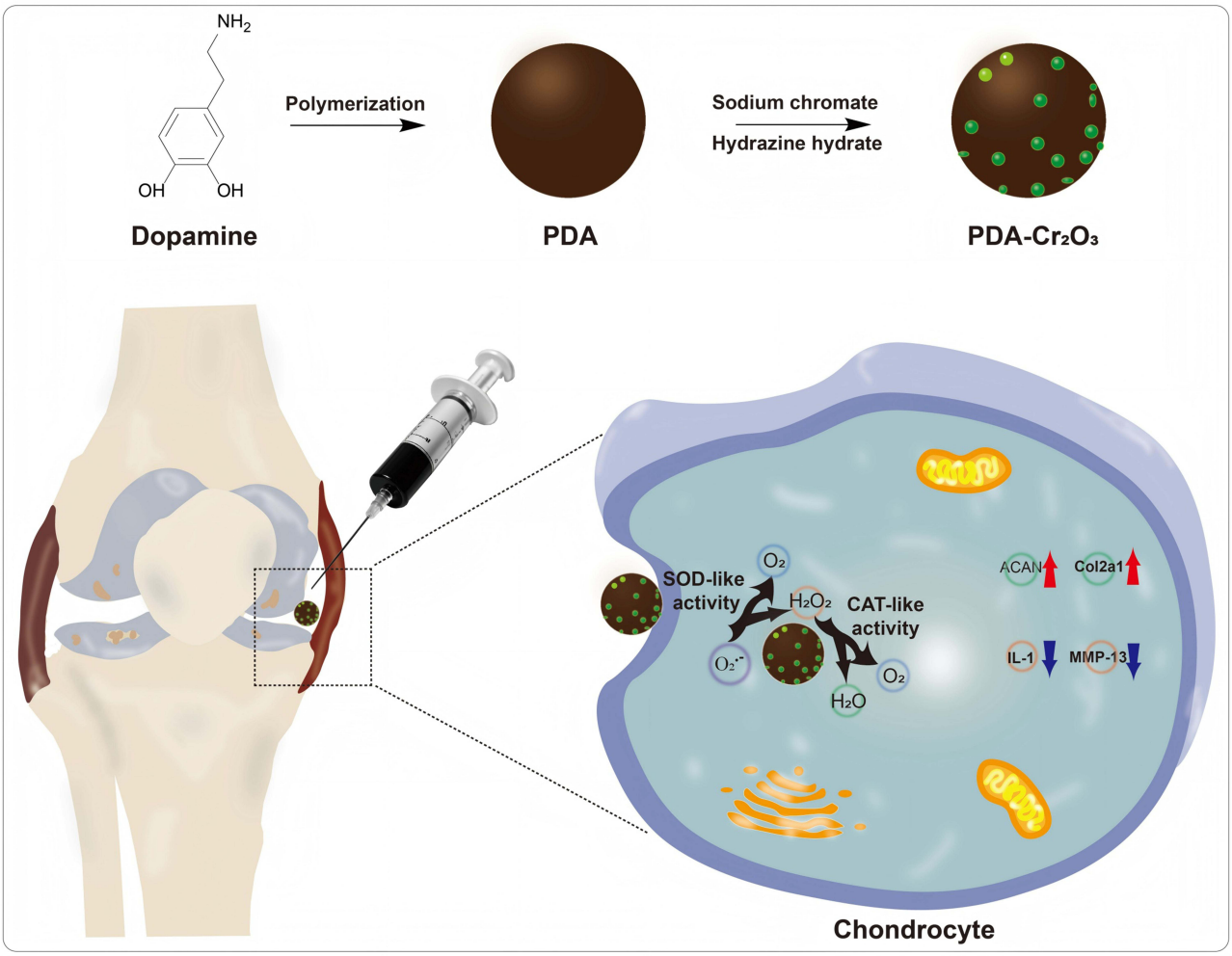

hydroxyl radicals (•OH).[6] Excessive ROS can cause progressive loss of cartilage matrix and apoptosis of chondrocytes.[7] Currently, ROS scavenging has become a crucial target for the treatment of OA. Researchers have developed multiple approaches to treat OA by scavenging ROS.

At present, ROS-scavenging drugs mainly include reducing agents, natural enzymes, and synthetic enzymes. As an excellent reducing agent, PDA has been widely used in various fields since it was first synthesized by Haeshin Lee in 2007.[8] He Zhao confirmed that PDA can effectively scavenge H_2O_2, and achieved good results in the treatment of acute peritonitis. Xingfu Bao demonstrated that PDA can efficiently scavenge $O_2^{\bullet-}$.[9] However, reducing agents will be rapidly consumed with the process of clearing ROS, requiring frequent administration, which brings great trouble to patients.

Since Lizeng Gao first developed the synthetic nanozyme Fe_3O_4 with peroxidase-like activity in 2007,[10] the synthetic nanozyme has made rapid development due to its low cost, suitability for mass production, and stable chemical properties. Although synthetic nanozymes have high enzyme activity, their application in the biomedical field is still limited. Synthetic nanozymes are mostly metals or metal oxides, which generally have disadvantages such as high cytotoxicity, easy agglomeration, difficult degradation, and difficulty entering cells.

Among many synthetic nanozymes, because of their high stability and high melting temperature, the Cr_2O_3 nanozyme gained extensive utilization in the field of catalysis.[11] Several studies have confirmed that Cr_2O_3 has good ROS scavenging ability.[11–13] However, as a synthetic nanozyme, Cr_2O_3 also has poor biocompatibility, which limits its

application in biological and medical fields, and several studies have attempted to modify Cr_2O_3 to improve its biocompatibility.[11,14] As a natural melanin analog, PDA is an excellent carrier and reducing agent. Based on the above reasons, we tried to combine PDA with Cr_2O_3 to construct a novel composite nanozyme to treat OA by scavenging ROS.

Materials and Methods

Materials

Sodium chromate was procured from Sigma Co., Ltd. Dopamine hydrochloride was procured by Shanghai Aladdin Co., Ltd. Ammonia solution (25%) was procured from Jinshan Chemical (Chengdu, China). Ethanol (99.7%) was procured from Sinopharm (Shanghai, China). Hydrazine hydrate was commercially obtained from Chuandong Chemical (Chongqing, China). Cy7 NHS ester was purchased from Yuanye Bio-Technology (Shanghai, China), and DMSO was purchased from Macklin Biochemical (Shanghai, China).

Synthesis of PDA

PDA was synthesized with reference to previous research (Figure 1A).[9] DI water (160 mL), ammonia solution (4 mL), and ethanol (80 mL) were mixed in a 500-mL flask. Then 20 mL volume of 0.05 g/mL dopamine hydrochloride aqueous solution was poured in dropwise and magnetic stirring (900 rpm) was continued for 24 h. Subsequently, the precipitation was gathered by centrifugation, followed by a wash with DI water. Finally, PDA powder was dried under a vacuum for 6 h after washing with alcohol. The final product was stored in a dry environment at 4°C.

Synthesis of PDA-Cr_2O_3

PDA-Cr_2O_3 was synthesized based on previous research (Figure 1A).[11,15,16] First, PDA nanoparticles (100 mg) were added into the blend of DI water (4 mL) and ethanol (80 mL) in a 500-mL flask, then 4 mL aqueous solution of sodium chromate (5 mg/mL) was added dropwise. At room temperature, the chemical reaction proceeded under magnetic stirring for 3 h. Then 320 μL hydrazine hydrate was added, then stirred the mixture for 2 h. Subsequently, the product was collected by centrifugation (10,000 rpm, 10 min).

Synthesis of Cy7-Labeled PDA-Cr_2O_3

The method for preparing Cy7-labeled PDA-Cr_2O_3 nanoparticles was adapted from previous studies with slight modifications.[17,18] Briefly, 5 mg of Cy7 NHS ester was dissolved in 9 mL of DMSO, and 2.5 mg of PDA-Cr_2O_3 nanoparticles were dispersed in 1 mL of deionized (DI) water. The two solutions were then mixed in a flask and stirred magnetically (900 rpm) in the dark for 4 h. Subsequently, the mixture was centrifuged at 10,000 rpm for 10 minutes to collect the precipitate. The precipitate was washed three times with a mixture of DMSO and DI water (9:1) to remove unreacted Cy7 NHS ester, resulting in purified Cy7-labeled PDA-Cr_2O_3 nanoparticles.

Characterization

The FTIR spectra were detected using an FTIR spectrometer (IRAffinity-1S, Shimadzu, Japan). X-ray diffractograms (XRD) were obtained using an X-ray diffractometer (Miniflex 600, Rigaku, Japan). The X-ray photoelectron spectroscopy (XPS) analysis was conducted on the nanomaterials by a Thermo ESCALAB 250Xi spectrometer. TEM images were obtained using a Hitachi microscope, and the particle size distribution was analyzed by analyzing the TEM pictures using ImageJ software. The energy dispersive X-ray (EDX) elemental mapping was obtained using an FEI Talos F200S field-emission microscope (USA). The zeta potential was detected utilizing a Malvern Nano-ZS analyzer (UK).

The Catalase-Like Activity of PDA-Cr_2O_3

Catalase facilitates the decomposition of H_2O_2 to O_2 and H_2O. When H_2O_2 is relatively sufficient, the stronger the activity of catalase is, the more H_2O_2 will be consumed. The remaining H_2O_2 can oxidize chromogenic substrate to generate N- (4-antipyryl) −3-chloro-5-atepbenzoquinonemonoimine by the catalysis of peroxidase. Based on this reason,

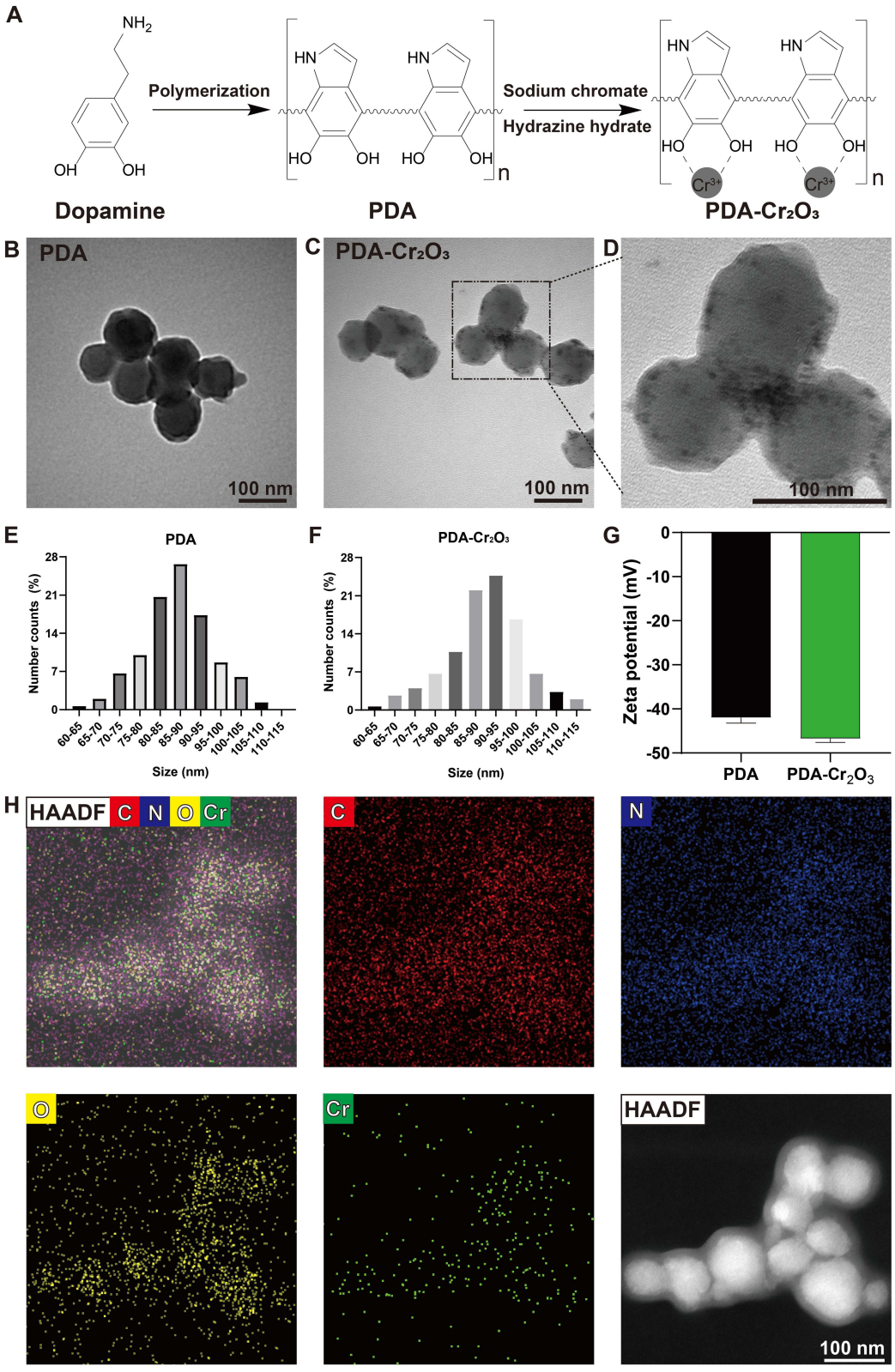

Figure 1 Schematic representation of the synthesis approaches and characterization of the nanoparticles. (**A**) The schematic diagram showing the synthesis methods of PDA and PDA-Cr_2O_3. (**B**) TEM micrograph of PDA. (**C** and **D**) TEM micrograph of PDA-Cr_2O_3. (**E**) Particle size distribution chart of PDA. (**F**) Particle size distribution chart of PDA-Cr_2O_3. (**G**) Zeta potentials of PDA and PDA-Cr_2O_3. (**H**) HAADF-STEM picture and elemental mapping pictures of PDA-Cr_2O_3 nanoparticle.

the catalase-like activity of PDA-Cr_2O_3 was examined using the catalase assay kit (Beyoime, China). We used the PDA solution and PDA-Cr_2O_3 solution to treat the working solution of the kit and then measured the absorbance at 520 nm. At last, we calculated the catalase activity according to the instructions.

The Stability of Catalase-Like Activity of PDA-Cr_2O_3

In order to detect the stability of the catalase-like enzymatic activity of PDA-Cr_2O_3 nanozyme in a harsh environment, we added the same quality of PBS, PDA, and PDA-Cr_2O_3 into 5 mL H_2O_2 solution (1 mol/L), respectively. Then we took photos to record the bubble production (O_2) at 0, 4, 12, and 24 h. To eliminate the interference of the retained bubbles, we vortexed the mixture 10 minutes before taking photos.

SOD-Like Activity of PDA-Cr_2O_3

WST-8 can interact with $O_2^{\bullet-}$ to generate formazan dye. And the SOD enzyme could facilitate the disproportionation reaction of $O_2^{\bullet-}$ to generate H_2O_2 and thus reduce the content of $O_2^{\bullet-}$. The stronger the enzyme activity of the SOD enzyme is, the less formazan dye will be generated, so the enzyme activity of the SOD enzyme can be calculated through colorimetric analysis. We used PDA solution and PDA-Cr_2O_3 solution to treat the working solution of the SOD assay kit (Beyotime, China), followed by measuring 450 nm absorbance. Then we calculated the SOD activity according to the instructions. We also tested the SOD-like ability of PDA-Cr_2O_3 by the electron spin resonance (ESR) method.

Extraction and Culture of Chondrocytes

The chondrocytes were isolated based on previous research.[19] First, the cartilage tissue was surgically extracted from the knee joints of Sprague-Dawley (SD) rats (3-day-old) in a sterile environment, and then the cartilage was diced into small chunks. The chunks were washed with saline containing 1% penicillin-streptomycin, and then the cartilage chunks were collected by centrifugation. Subsequently, the cartilage chunks were disintegrated in 0.25% trypsin-EDTA solution (Biosharp, China) for half an hour. Afterwards, the precipitates were collected by centrifugation. Next, the precipitates were incubated in type II collagenase solution (37°C, 3 h). The enzymatically digested mixture was briefly centrifuged (1000 rpm, 5 s) to isolate the supernatant, and then the supernatant was centrifuged (1000 rpm, 5 min) to collect the precipitates (chondrocytes). Subsequently, the isolated chondrocytes were cultured using DMEM complete medium. When the chondrocytes grew to nearly 80–90% confluency, they were passaged and the second generation of cells was employed for the following cell experiments.

Cytotoxicity Test

The cytotoxicity of PDA and PDA-Cr_2O_3 was determined by the cell proliferation-toxicity assay kit (CCK-8, Biosharp, China). In brief, the chondrocytes were plated into 96-well plates. After 1 day, the media were replaced with 180 μL complete DMEM medium that contained PDA or PDA-Cr_2O_3 at multiple concentrations. After 1 day, the medium of each well was supplanted by 180 μL DMEM medium and 20 μL CCK-8. The 450 nm absorbance was quantified after a 2-hour incubation.

Detection of the ROS Level in Chondrocytes

The ROS detection kit (Beyotime, China) was utilized to measure the ROS scavenging ability of the nanoparticles in OA chondrocytes. Briefly, there were 4 groups: normal group, OA group, PDA group, and PDA-Cr_2O_3 group. Chondrocytes were placed into 6-well culture plates (1×10^6 cells/well), accompanied by 2 mL complete DMEM medium. Eight hours later, the medium of the normal group was substituted by 2 mL fresh complete DMEM medium, and the media of the other three groups were substituted by 2 mL complete DMEM medium, accompanied by recombinant human IL-1β (10 ng/mL). After 1 day, all wells were washed twice with PBS solution. Complete DMEM medium (2 mL) was added to every well of the normal group and OA group. The wells of the other two groups were infused with 2 mL complete DMEM medium containing 50 μg/mL PDA or PDA-Cr_2O_3. After 24 h, chondrocytes were treated with the 2′,7′-Dichlorodihydrofluorescein diacetate (DCFH-DA) probes (10 μM) for 20 min in conditions of darkness. Following this,

unloaded DCFH-DA was rinsed away using PBS solution, and fluorescent pictures were captured utilizing a fluorescence microscope.

The Detection of Intracellular $O_2^{\bullet-}$ Level

We detected the ability of PDA and PDA-Cr_2O_3 to clear intracellular $O_2^{\bullet-}$ using the dihydroethidium (DHE) fluorescent probe (Beyotime, China). The chondrocytes received the aforesaid treatment. Then the chondrocytes were treated with DHE (10 μM) in an incubator for 30 min in the dark. Unloaded DHE was washed off using PBS solution, and images were taken by a fluorescence microscope.

Quantitative Real-Time PCR

The chondrocytes were partitioned into 4 experimental groups: normal group, OA group, PDA group, and PDA-Cr_2O_3 group. Chondrocytes were seeded into 12-well culture plates (1×10^6 cells/well density), accompanied by 1 mL complete DMEM medium. Twenty-four hours later, the medium was removed. Each well in the normal group received 1 mL complete DMEM culture medium. Each well in the other three groups was added with 1 mL of complete DMEM medium and recombinant human IL-1β (10 ng/mL). After 24 hours, the medium of each well was substituted with 1 mL of different media: 1) normal group: complete DMEM medium; 2) OA group: complete DMEM medium; 3) PDA group: complete DMEM medium and 50 μg PDA; 4) PDA-Cr_2O_3 group: complete DMEM medium and 50 μg PDA-Cr_2O_3. Twenty-four hours later, the cell culture supernatants were harvested for subsequent enzyme-linked immunosorbent assay (ELISA) experiments, and total RNA was retrieved by an RNA extraction kit (Magen, China) and reverse-transcribed subsequently. Finally, the PCR analysis was performed using a PCR device (LightCycler96, Roche, Switzerland). Relative mRNA abundance was assessed via the $2^{-\Delta\Delta Cq}$ method and calibrated by a housekeeping gene GAPDH. Table S1 presents the specific primer sequences.

ELISA Experiments

The protein expression of the biomarker MMP-13 and Col2a1 within the harvested cell culture supernatants as described above were assessed via ELISA. The level of MMP-13 protein was examined utilizing a rat MMP-13 ELISA kit (Solarbio, China). The protein concentration of Col2a1 was subsequently tested using the rat Col2a1 ELISA kit (Zeye China).

Live/Dead Staining

To examine the cytoprotective effects of nanoparticles on OA chondrocytes, live/dead staining was done by the employment of the Calcein-AM/PI double staining kit (Beyotime, China). The induction of OA chondrocytes and the treatment were the same as described above. The chondrocytes were incubated with both Calcein-AM (1 μM) and PI (1 μM) for 5 minutes at 37°C. Then the photographs were captured with a fluorescence microscope. Quantitative analysis of the rate of chondrocyte apoptosis was performed using ImageJ software.

The Establishment of the OA Model

A total of 24 male SD rats (150–200g) were utilized in OA treatment studies. All animal experiments were examined and approved by the Ethics Committee of Xiangyang Central Hospital (NO. 2021-108-002). All rats were placed in a clean-grade room and provided unrestricted access to standard food and water. The experimental OA animal model was constructed through anterior cruciate ligament transection (ACLT) surgery.[20] All rats were arbitrarily divided into 4 experimental groups (n=6): 1) sham group; 2) OA group; 3) PDA group; 4) PDA-Cr_2O_3 group. All rats of the sham group underwent sham surgeries. Briefly, the rats were anesthetized. Then the skins of the knee joints were disinfected with povidone-iodine after shaving. The joint capsules of the knee were sutured immediately after they were incised without any additional manipulation. The rats of the other three experimental groups were modeled by the ACLT procedure. In brief, the skin and capsule of the joint were incised along the medial side. Subsequently, the anterior cruciate ligament was severed. Then the anterior drawer test was administered to check whether the anterior cruciate

ligament had been successfully transected. Subsequently, the joint capsule and skin were sutured. At last, each rat underwent an intramuscular administration of penicillin sodium (160,000 U) for 3 consecutive days.

In vivo Imaging and Assay

To evaluate the retention time of PDA-Cr_2O_3 nanoparticles in the joint and their systemic distribution following intra-articular injection, Cy7-labeled PDA-Cr_2O_3 nanoparticles were injected into the knee joints of rats. Fluorescence images and the corresponding mean fluorescence intensity at the knee joint were acquired at predetermined time points using a small animal in vivo imaging system (Fusion FX, Vilber, France).

Treatment of OA in Rats

Thirty days after the surgery, the administration via intra-articular injection was conducted every 3 days for 4 or 8 consecutive weeks. The specific treatment regimens were as follows: (1) sham group: no treatment; (2) OA group: 100 μL normal saline solution; (3) PDA group: 100 μL PDA solution (50μg/mL); (4) PDA-Cr_2O_3 group: 100μL PDA-Cr_2O_3 solution (50μg/mL).

Toxic Effects on Major Organs

All rats were euthanized after treatment for 4 weeks or 8 weeks. Afterwards, the knee joints of all rats were gathered and stored at −80°C. One rat from each group was selected randomly and its heart, lung, liver, spleen, and kidneys were collected. Subsequently, these organs were immediately immersed in 4% paraformaldehyde for 48 hours for fixation. The organs were then dehydrated, embedded, sectioned, and histologically dyed using the hematoxylin-eosin (HE) protocol. Furthermore, the toxic effects of nanoparticles were assessed by observing the internal structures of the major organs.

The Gross Evaluation of the Knee Joints

The changes of the joints were assessed by three independent observers blinded to treatment group assignment according to the method described by Pelletier.[21] Specifically, the erosion depth of articular cartilage of the knee joint was graded from 0 to 4 level (4 = the subchondral bone was eroded, 3 = erosion reaching the deep layer, 2 = erosion extending to the intermediate layer, 1 = mild fibrosis or yellowish discoloration, and 0 = normal appearance). The observers assessed the medial plateau, lateral plateau, medial condyle, and lateral condyle separately. The gross macroscopic score was the average score of the lateral condyle and medial condyle plus the average score of the lateral plateau and the medial plateau.

The Histological Evaluation

The knee joints were immersed in 4% paraformaldehyde for 24 h. Subsequently, the joints were decalcified by immersion in EDTA solution (0.5 M) for 1 month. Subsequently, they were dehydrated, embedded, and sectioned. Then the sections were dyed using safranin-O/fast green and hematoxylin-eosin staining protocols. Finally, according to OARSI standards, the sections were pathologically evaluated by three observers with no knowledge of the experimental grouping.

Statistical Analysis

Statistical analysis was performed using IBM SPSS software. All graphs were created using OriginPro 2021 or GraphPad Prism 8.0.1 software. Results from three independent experiments were presented as the mean ± standard deviation after statistical processing. P values less than 0.05 were considered statistically significant. *# indicates $p < 0.05$; * * and # # said $p < 0.01$; ***### indicates $p < 0.001$; ns indicates no significant.

Results

Characterization of PDA and PDA-Cr_2O_3

First of all, we synthesized PDA nanoparticles. As shown in Figure 1B, PDA was spherical nanoparticles with a uniform particle size. The mean particle size of PDA was 86.90 nm (Figure 1E). Subsequently, we synthesized PDA-Cr_2O_3 based

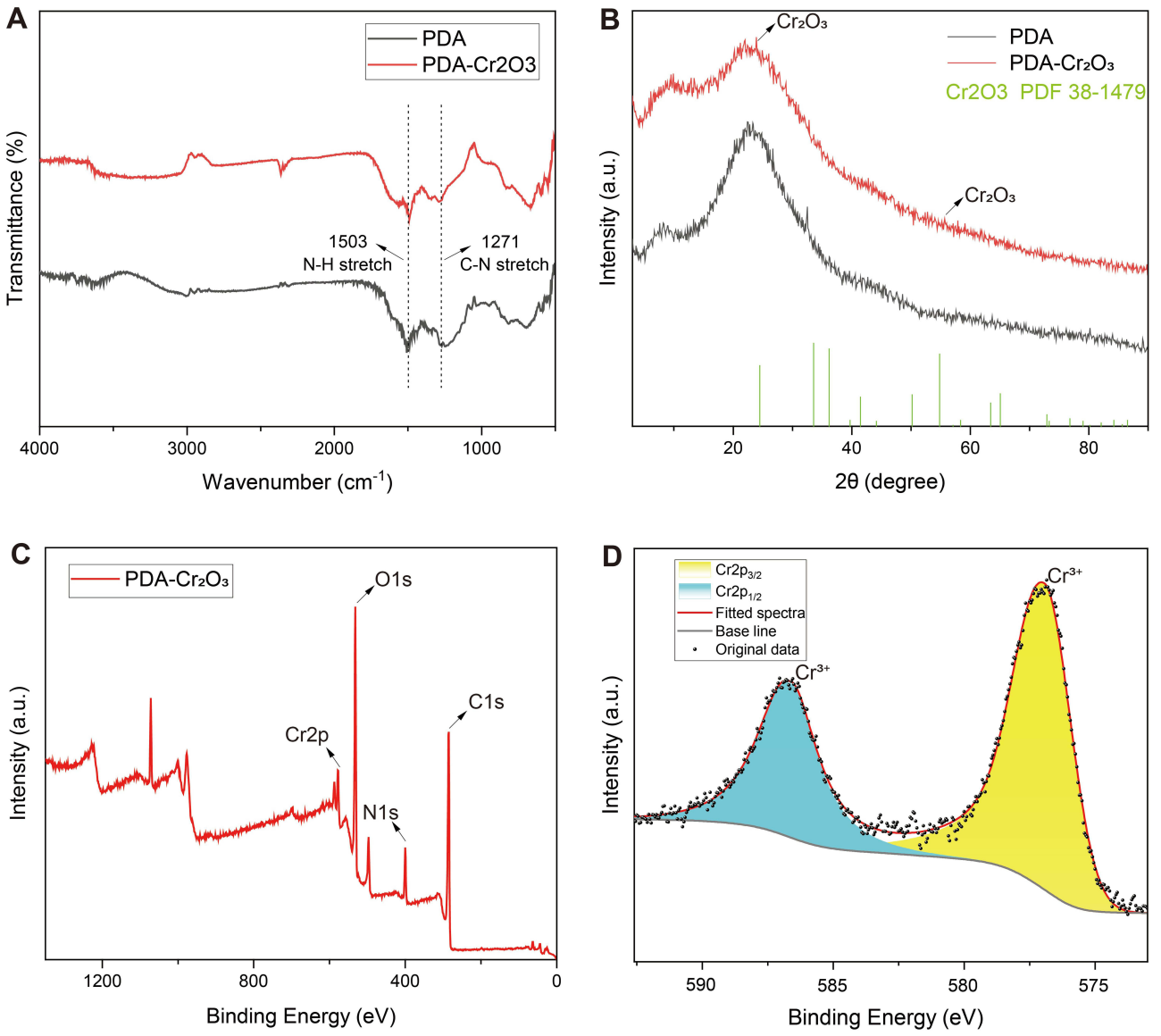

Figure 2 Characterization analysis of the PDA and PDA-Cr_2O_3 nanoparticles. (**A**) FTIR spectra of the nanoparticles. (**B**) XRD patterns of PDA and PDA-Cr_2O_3. (**C**) Full XPS spectrum of PDA-Cr_2O_3. (**D**) Cr2p high-resolution XPS spectrum of PDA-Cr_2O_3.

on PDA, as shown in Figure 1C, the surface of PDA was loaded evenly with tiny Cr_2O_3 nanoparticles (Figure 1D), and the mean particle size of PDA-Cr_2O_3 was 90.12 nm (Figure 1F). The zeta potential belonging to PDA was −41.97 mV, while that of PDA-Cr_2O_3 was −46.73 mV (Figure 1G). As shown in Figure 1H, a homogeneous deposition of Cr elements on the surface of PDA was observed in TEM elemental mapping images.

The FTIR spectra are presented in Figure 2A, the stretching vibration peak of the C-N bond can be seen at 1271 cm^{-1} and the N-H stretching vibration characteristic peak can be observed at 1503 cm^{-1}. These peaks are the characteristic peaks of PDA.[22] In the XRD spectrum of PDA-Cr_2O_3 (Figure 2B), distinct XRD peaks could be observed at 2θ = 23.9, 55.2, which corresponded to Cr_2O_3 compared with the standard card. The XPS spectra were applied to explore the chemical element composition of the materials. The full-scale XPS spectrum is depicted in Figure 2C, and the characteristic peaks of Cr, O, C, and N elements can be observed. Subsequently, in order to clarify the valence state of the Cr element, the XPS spectroscopy with high resolution for Cr2p was performed (Figure 2D). The peaks located at 576.9 eV and 586.6 eV belong to Cr2p3/2 and Cr2p1/2 of Cr_2O_3, respectively. This indicates that the Cr element in the nanomaterial exists in the form of Cr_2O_3.[12] The above results confirm that we have successfully synthesized PDA and PDA-Cr_2O_3.

The Cytotoxicity and the Toxicity in vivo

We first tested the cytotoxicity of nanomaterials on chondrocytes using a cell proliferation-toxicity assay kit (CCK-8). PDA had low toxicity at a concentration of 50 μg/mL, with the survival rate of chondrocytes higher than 90% (Figure 3A). The toxicity of PDA-Cr_2O_3 was slightly higher, at the concentration of 50 μg/mL, the survival rate was still higher than 90% (Figure 3B).

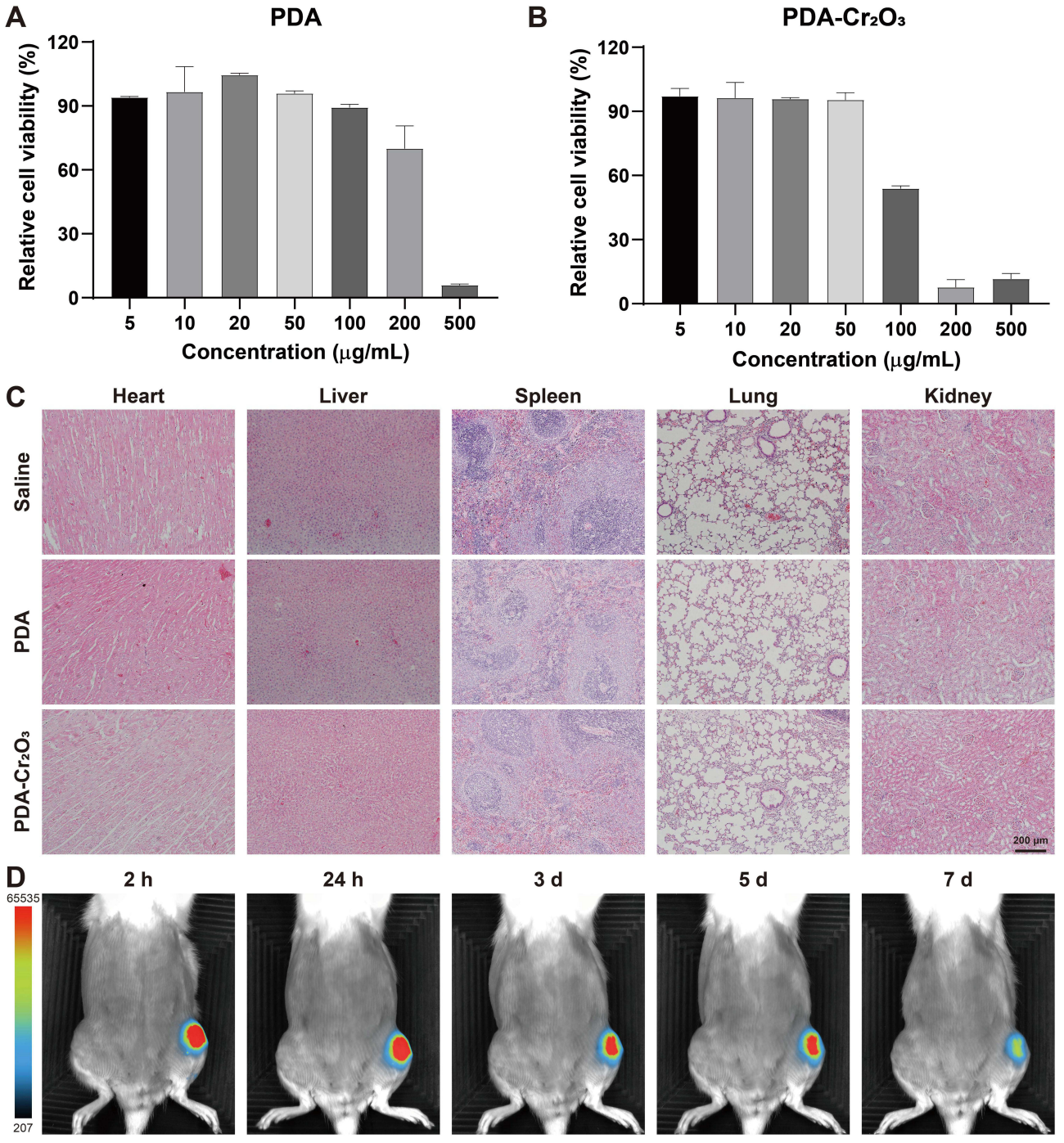

Figure 3 Toxicity studies of PDA and PDA-Cr_2O_3 nanoparticles, and in vivo imaging of Cy7-labeled PDA-Cr_2O_3 nanoparticles. (**A**) Cytotoxicity of PDA. (**B**) Cytotoxicity of PDA-Cr_2O_3. (**C**) HE staining of viscera in SD rats. Scale bar: 200 μm. (**D**) In vivo fluorescence imaging of rats following intra-articular injection of Cy7-labeled PDA-Cr_2O_3 nanoparticles at designated time points.

https://doi.org/10.2147/IJN.S538289

The most prevalent toxic side effect of drugs is visceral toxicity.[23] We observed and evaluated the HE pathological sections of rat viscera after medication. No significant injury abnormalities were observed in the main visceral organs of the PDA and PDA-Cr_2O_3 groups. PDA-Cr_2O_3 at therapeutic doses had no obvious viscerotoxic effects (Figure 3C).

The Retention and Clearance of Nanoparticles in the Joint

As shown in Figure 3D, The in vivo imaging study in SD rats revealed that Cy7-labeled PDA-Cr_2O_3 nanoparticles exhibited significant retention within the joint, with fluorescence signals still detectable on day 7 post-injection. This indicates that the nanoparticles can remain in the joint for an extended period. At the same time, the fluorescence intensity gradually decreased over time, suggesting that the nanoparticles are slowly being cleared from the joint. This finding supports the potential of PDA-Cr_2O_3 nanoparticles to provide sustained therapeutic effects in osteoarthritis treatment.

Moreover, no significant fluorescence signals were detected in the body, other than the knee joint, throughout the study. This is mainly due to the minimal treatment dose of Cy7-labeled PDA-Cr_2O_3 nanoparticles, which were largely retained in the knee joint, along with their slow metabolic clearance, resulting in limited impact on other body parts, including internal organs.

The Catalytic-Like Activity of PDA-Cr_2O_3

The H_2O_2 scavenging capabilities of PDA and PDA-Cr_2O_3 were assessed using a catalase assay kit. PDA had a certain extent of H_2O_2 scavenging ability with a scavenging rate of 16.45%, and the H_2O_2 scavenging rate by PDA-Cr_2O_3 increased to 25.20% (Figure 4B).

The catalytic stability of enzyme in harsh conditions is a key index for assessing the quality of an enzyme. As shown in Figure 4A, PDA-Cr_2O_3 nanozyme could rapidly exhibit catalase-like activity in the H_2O_2 solution (1mol/L), decomposing H_2O_2 to produce a large number of O_2 bubbles and it still maintained high catalase-like activity after 24 h. PDA-Cr_2O_3 nanozyme can maintain high catalase-like activity for a long time after exposure to high concentrations of oxidant.

The SOD-Like Activity

The capacity to scavenge $O_2^{\bullet-}$ was evaluated utilizing a superoxide dismutase assay kit. As shown in Figure 4C, PDA exhibited the ability of $O_2^{\bullet-}$ clearance, with an inhibition ratio of 16.65%, and the corresponding clearance effect of PDA-Cr_2O_3 on $O_2^{\bullet-}$ was significantly improved to 27.37%. In addition to the kit, similar results were obtained by the ESR method. As shown in Figure 4D, PDA-Cr_2O_3 could substantially reduce the ESR signal intensity of $O_2^{\bullet-}$, indicating that PDA-Cr_2O_3 could effectively remove $O_2^{\bullet-}$.

Intracellular $O_2^{\bullet-}$ Scavenging Ability of the Nanoparticles

We also tested the activity of PDA-Cr_2O_3 to scavenge $O_2^{\bullet-}$ in inflammatory chondrocytes using the $O_2^{\bullet-}$ probe DHE, the outcomes are depicted in Figure 4F. The mean fluorescence intensity reflecting the content of $O_2^{\bullet-}$ was quantified by ImageJ software, with the results presented in Figure 4E. There was only a small amount of $O_2^{\bullet-}$ in normal chondrocytes, while those in OA chondrocytes increased significantly. PDA could remove part of $O_2^{\bullet-}$, while PDA-Cr_2O_3 substantially scavenged $O_2^{\bullet-}$ in inflammatory chondrocytes to a level close to that of normal chondrocytes.

Intracellular Total ROS Scavenging Ability

To assess the total ROS scavenging capacity in the physiological environment, the ROS-sensitive fluorescent probe DCFH-DA was employed to quantify the intracellular total ROS levels. Compared with the normal chondrocytes, the inflammatory chondrocytes (OA group) had significantly increased ROS levels (Figure 4G). The fluorescence intensity dropped significantly in the PDA and PDA-Cr_2O_3 groups. Subsequently, the mean fluorescence intensity was quantified by the ImageJ software (Figure S1). The mean fluorescence intensity was 21.90 in the normal group, 127.92 in the OA group, 85.97 in the PDA group, and 47.94 in the PDA-Cr_2O_3 group. Thus, PDA-Cr_2O_3 could significantly decrease the ROS levels in the inflammatory chondrocytes. The abnormal overproduction of endogenous ROS in cartilage tissue is an

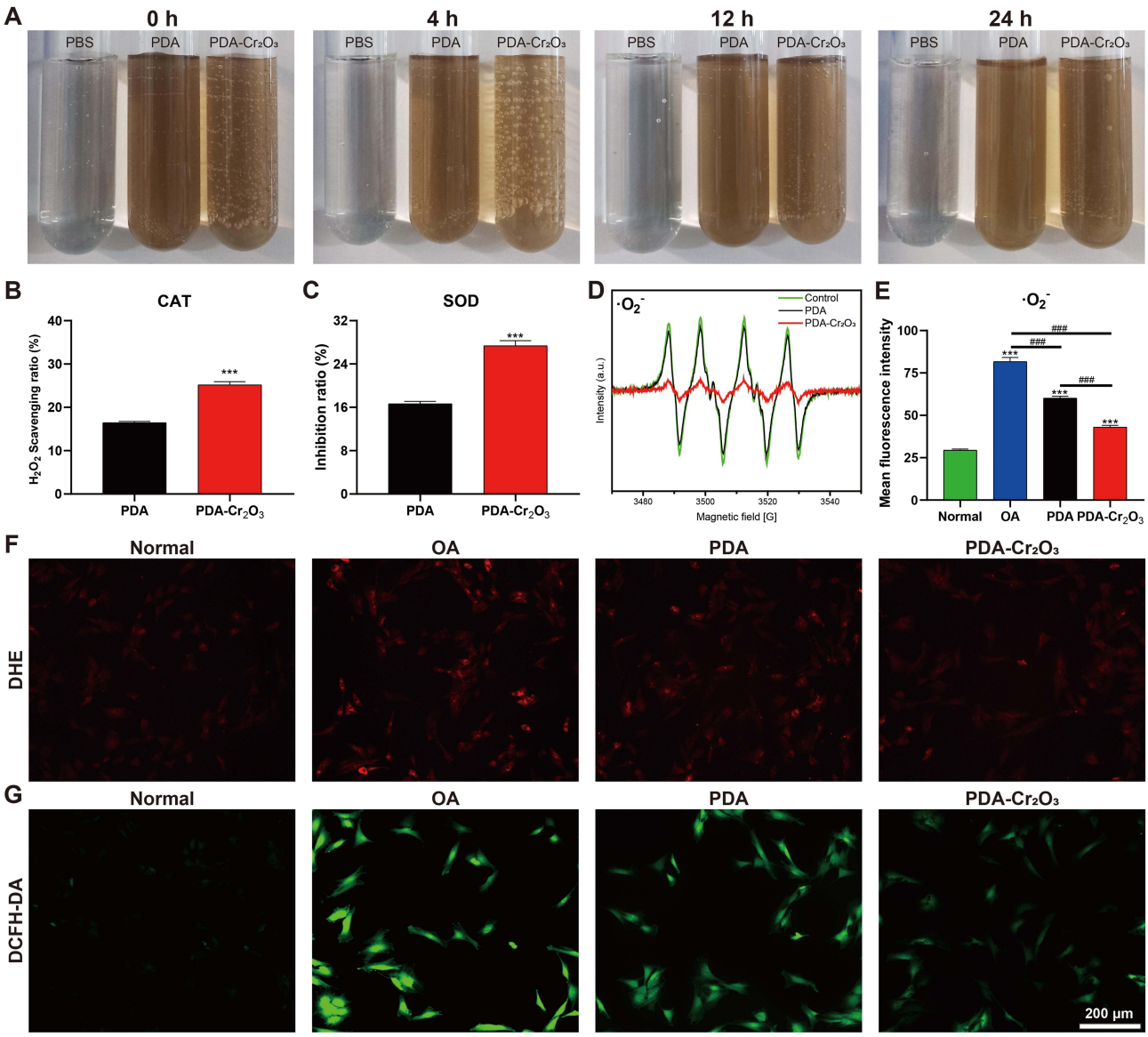

Figure 4 ROS scavenging capacity of PDA and PDA-Cr_2O_3. (**A**) The steadiness of catalase-like activity of PDA-Cr_2O_3 nanozyme. (**B**) H_2O_2 scavenging ability of the nanoparticles. The * symbol indicates the comparison between two groups, with *** representing $p < 0.001$. (**C**) $O_2^{\bullet-}$ scavenging capacity tested by the detection kit. The * symbol indicates the comparison between two groups, with *** representing $p < 0.001$. (**D**) $O_2^{\bullet-}$ scavenging ability measured by ESR methods. (**E**) The quantification of mean fluorescence intensity of $O_2^{\bullet-}$ probe (DHE) in chondrocytes. The * symbol indicates comparisons between the normal group and all other groups, while the # symbol represents pairwise comparisons among the remaining groups. *** and ### indicate $p < 0.001$. (**F**) $O_2^{\bullet-}$ content in living chondrocytes was detected by the DHE probe. (**G**) ROS content in living chondrocytes was determined by the DCFH-DA probe. Scale bar: 200 μm.

important hallmark of OA.[24] ROS can induce direct oxidative damage to cellular DNA and proteins, ultimately triggering chondrocyte apoptosis. After chondrocyte apoptosis, the cellular contents are liberated into the extracellular environment, and then a large number of new ROS are produced, thus forming a vicious cycle.[25] The oxidative stress injury induced by ROS can lead to progressive cartilage damage.[26]

The Situation of Gene Expression

To explore the influence of PDA and PDA-Cr_2O_3 on the gene expression of inflammatory chondrocytes, we measured the relative mRNA expression levels of chondrocytes by qRT-PCR. As shown in Figure 5A, we first measured the expression levels of the IL-1 gene, and the IL-1 mRNA content of the inflammatory chondrocytes (OA group) was 218.57 times as much as that of the normal group, which decreased to 108.31 times after PDA treatment and substantially to 1.58 times

https://doi.org/10.2147/IJN.S538289

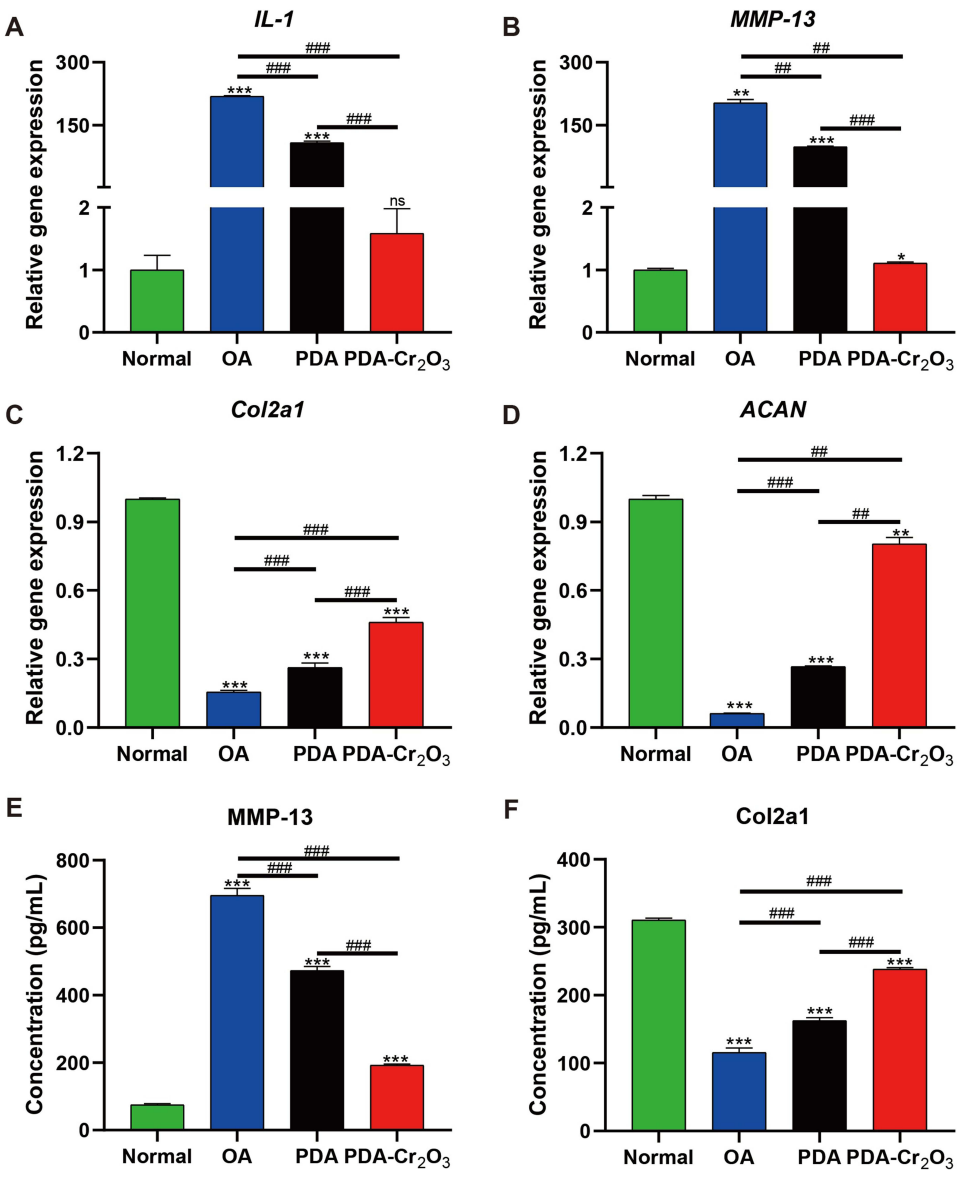

Figure 5 The expressions of four key genes validated by qRT-PCR and two key proteins measured by ELISA. (**A**) qRT-PCR result of IL-1. (**B**) qRT-PCR result of MMP-13. (**C**) qRT-PCR result of Col2a1. (**D**) qRT-PCR result of ACAN. (**E**) MMP-13 protein expression measured using ELISA. (**F**) Col2a1 protein expression measured by ELISA. The * symbol indicates comparisons between the normal group and all other groups, while the # symbol represents pairwise comparisons among the remaining groups. * indicates $p < 0.05$; ** and ## said $p < 0.01$; ***, ### indicates $p < 0.001$; ns indicates no significant.

after PDA-Cr_2O_3 treatment. The matrix metalloproteinases (MMPs) can decompose the extracellular matrix of cartilage and have crucial impacts on the onset and development of OA. Among them, MMP-13 is quite important. In our results (Figure 5B), in comparison with the normal group, the transcriptional level of MMP-13 mRNA in OA chondrocytes was significantly higher. PDA-Cr_2O_3 could significantly reduce the transcriptional level of MMP-13, which was almost equal to the level of the normal group. In addition, we detected the characteristic genes of the chondrocytes (Col2a1 and ACAN). As exhibited in Figure 5C and D, the level of Col2a1 mRNA in OA chondrocytes was only 15.51% of that in the normal chondrocytes, which experienced a significant increase subsequent to the treatment with PDA and PDA-Cr_2O_3. The regulation of ACAN gene expression was similar to that of Col2a1.

IL-1 is of crucial importance in the onset and progression of OA.[27] IL-1 inhibits the expression of the major ECM constituents (proteoglycans and type II collagens) and promotes the expression of a series of proteolytic enzymes, for example, MMP-13, ADAMTS-4, and MMP-1, promoting the catabolism of the ECM.[28,29] In addition, IL-1 upregulates

the expression of various inflammatory cytokines, for example, IL-6 and IL-8.[30] Furthermore, IL-1 has the capacity to trigger the generation of ROS.[31] Only trace amounts of H_2O_2 were present in normal chondrocytes, but the concentration of H_2O_2 was notably increased in inflammatory chondrocytes induced by IL-1β.[32,33] Previous studies found that the protein content of IL-1β rose substantially in the synovial fluid of OA patients.[34] This study also confirmed that the gene transcriptional level of IL-1 was substantially upregulated in OA chondrocytes.

The Situation of Protein Expression

We also detected the expression of the inflammation-related protein (MMP-13) and the chondrocyte-characteristic protein (Col2a1) by the ELISA method. The abundance of MMP-13 protein in the normal group was extremely low (74.77 pg/mL), which in the OA group markedly rose to 695.80 pg/mL. It was 472.71 pg/mL and 192.47 pg/mL in the PDA and PDA-Cr_2O_3 groups, respectively (Figure 5E). However, the expression situation of the Col2a1 protein exhibited significant differences. Compared with the normal group (310.54 pg/mL), the expression of Col2a1 protein in the OA group decreased to 115.37 pg/mL which was increased to 238.03 pg/mL in the PDA-Cr_2O_3 group (Figure 5F). PDA-Cr_2O_3 can decrease the expression of some inflammatory proteins and upregulate the expression of some functional proteins in chondrocytes.

The Protective Function of PDA-Cr_2O_3 on OA Chondrocytes

Live/dead staining was utilized to appraise the protective influence of nanoparticles on inflammatory chondrocytes. As shown in Figure 6, there were only a few dead chondrocytes (red) in the normal group, while a great many dead chondrocytes were discovered in the OA group. After treatment with PDA and PDA-Cr_2O_3, the proportion of dead chondrocytes decreased significantly. After analysis using ImageJ software (Figure S2), the apoptosis ratio of OA chondrocytes was 16.24%, and after treatment with PDA-Cr_2O_3, the apoptosis ratio of chondrocytes could be reduced to 3.04%. PDA-Cr_2O_3 could effectively cure OA chondrocytes.

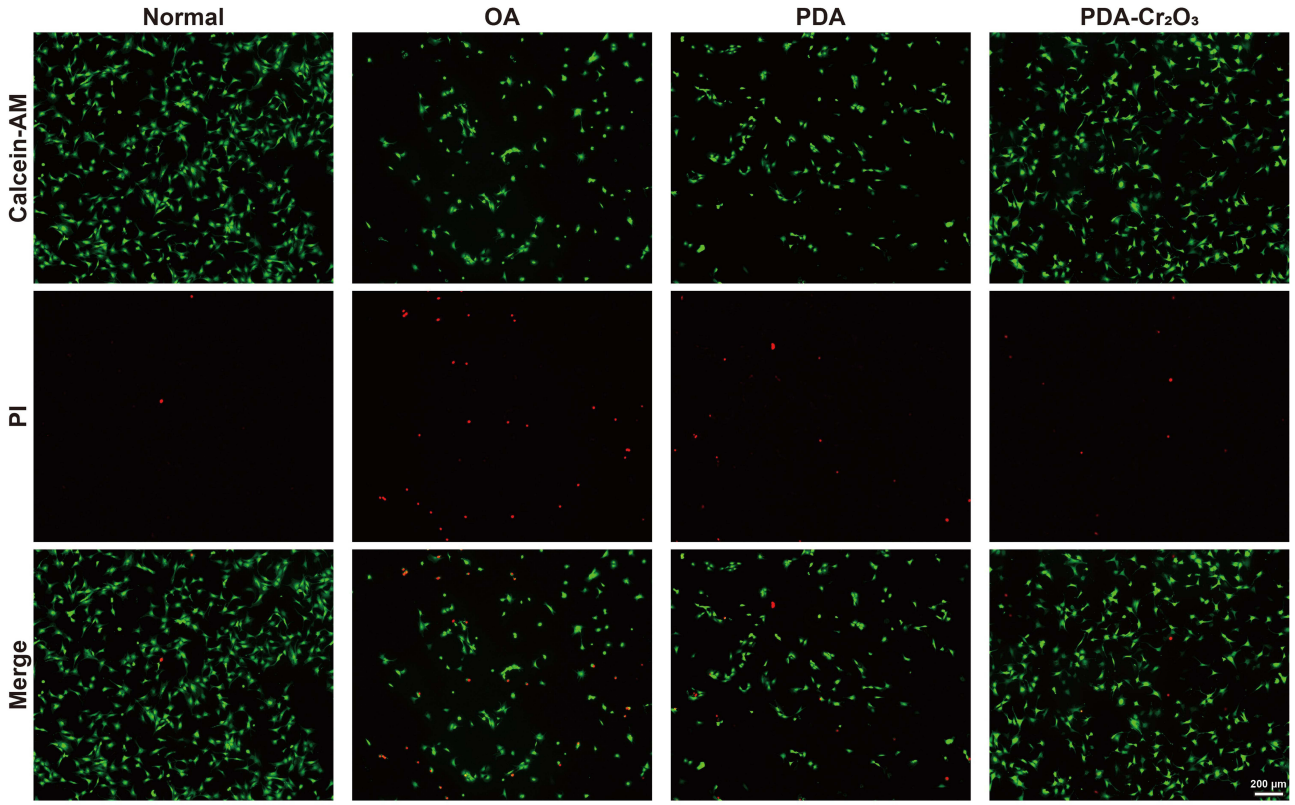

Figure 6 Live/dead staining. Fluorescent images of live/dead chondrocytes in different groups. Green: live chondrocytes; red: dead chondrocytes. Scale bar: 200 μm.

https://doi.org/10.2147/IJN.S538289

The Therapeutic Effect in vivo

At the 4-week and 8-week endpoints, the knee joints were harvested, and the gross appearances of the joints were presented in Figure 7A and B. In the sham group, the surface of the articular cartilage was intact. In comparison, the knee joints of the OA group showed typical osteoarthritic features, with rough irregular articular surfaces and eroded articular cartilage matrix. After treatment with PDA and PDA-Cr_2O_3, the knee joint lesions were significantly alleviated. In the PDA-Cr_2O_3 group, there were almost no defects on the surface of the cartilage and no erosions in the cartilage matrix, and the appearance was similar to the sham group. Subsequently, the macroscopic score was evaluated referring to Pelletier's study. As shown in Figure 7C, after a treatment duration of 4 weeks, the macroscopic score of the OA group was 3.78, which was substantially higher compared to the sham group (1.17). After the treatment with PDA and PDA-Cr_2O_3, the scores decreased to 3.44 and 1.44, respectively. After a treatment duration of 8 weeks, the macroscopic score of the OA group was 4.67, which was substantially higher compared to the sham group (1.39). After the treatment with PDA-Cr_2O_3, the scores decreased to 1.56 (Figure 7D). The macroscopic score of the PDA-Cr_2O_3 group approximated that of the sham group.

At last, the tissue sections of the knee joints were independently processed with HE and safranin-O/fast green staining protocols. The microscopic appearances of the joints were shown in Figure 8A and B, in the sham group, the articular cartilage surface was nearly intact, with mild abrasion in some small regions. The articular cartilage matrix was nearly intact, with a small amount of microscopic cracks in the superficial zone, without vertical fissures and cartilage erosion. However, the knee joints of the OA group showed typical osteoarthritic changes, with densely packed fissures and defects on the surface of the articular cartilage. There were a large number of vertical fissures and large-area cartilage erosion in the matrix. Local subchondral bone was exposed and the bone surface was repaired by fibrocartilage. Compared with the OA group, there were different degrees of relief in each treatment group, especially in the PDA-Cr_2O_3 group, and the pathological findings of the knee joints were close to those in the sham group. There were a few discontinuities on the articular cartilage surface and a small amount of matrix cracks in the focal cartilage superficial zone. To standardize the comparison of the treatment effects, then we performed the osteoarthritis pathological score according to the OARSI criteria. As shown in Figure 8C, after a treatment duration of 4 weeks, the OARSI score of the sham group was only 0.89, while the score of the OA group increased substantially to 9.33, and the score of the PDA and PDA-Cr_2O_3 group decreased to 8.00 and 2.78. These findings collectively demonstrate that PDA-Cr_2O_3 had a good therapeutic effect on OA. After a treatment duration of 8 weeks, the OARSI score of the OA group was 10.44, which significantly surpassed the score (0.67) of the sham group. After the treatment with PDA-Cr_2O_3, the scores decreased to 2.44 (Figure 8D).

Discussion

There are currently about 300 million people with OA worldwide. OA has emerged as a leading cause of incapacity in the aged due to pain and loss of function.[35] In spite of the high incidence of OA and the numerous studies, the drugs clinically used, for example, non-steroidal anti-inflammatory drugs (NSAIDs) and corticosteroids, can only relieve symptoms, such as pain, swelling, and stiffness, rather than reverse and cure the disease.[36] Theoretically, if effective intervention is performed in the initial and intermediate stages of OA, it may prevent or delay the development of OA and decrease the likelihood of having joint replacement surgery.

The onset and progression of OA are closely related to excessive ROS in the joint microenvironment. Oxidative stress induced by excessive ROS leads to chondrocyte apoptosis by damaging mitochondrial DNA and proteins in chondrocytes. In addition, excessive ROS can also induce cartilage degradation and destruction by inhibiting ECM formation and promoting ECM catabolism.[37] ROS scavenging has become a significant approach for OA treatment. Recent researches show that various antioxidant defense strategies could effectively keep the intracellular redox equilibrium and shield cells from oxidative stress injury.[9] According to the different mechanisms of ROS scavenging, there are three categories of ROS scavenging drugs, which are reducing agents, natural enzymes, and synthetic nanozymes.

There are a large number of natural reducing agents, which can directly reduce ROS through redox reactions. Among those reducing agents, due to its excellent biocompatibility and ROS scavenging ability, PDA has garnered a great deal of attention. PDA has excellent biocompatibility and is now recognized as having low cytotoxicity.[38] PDA is an excellent

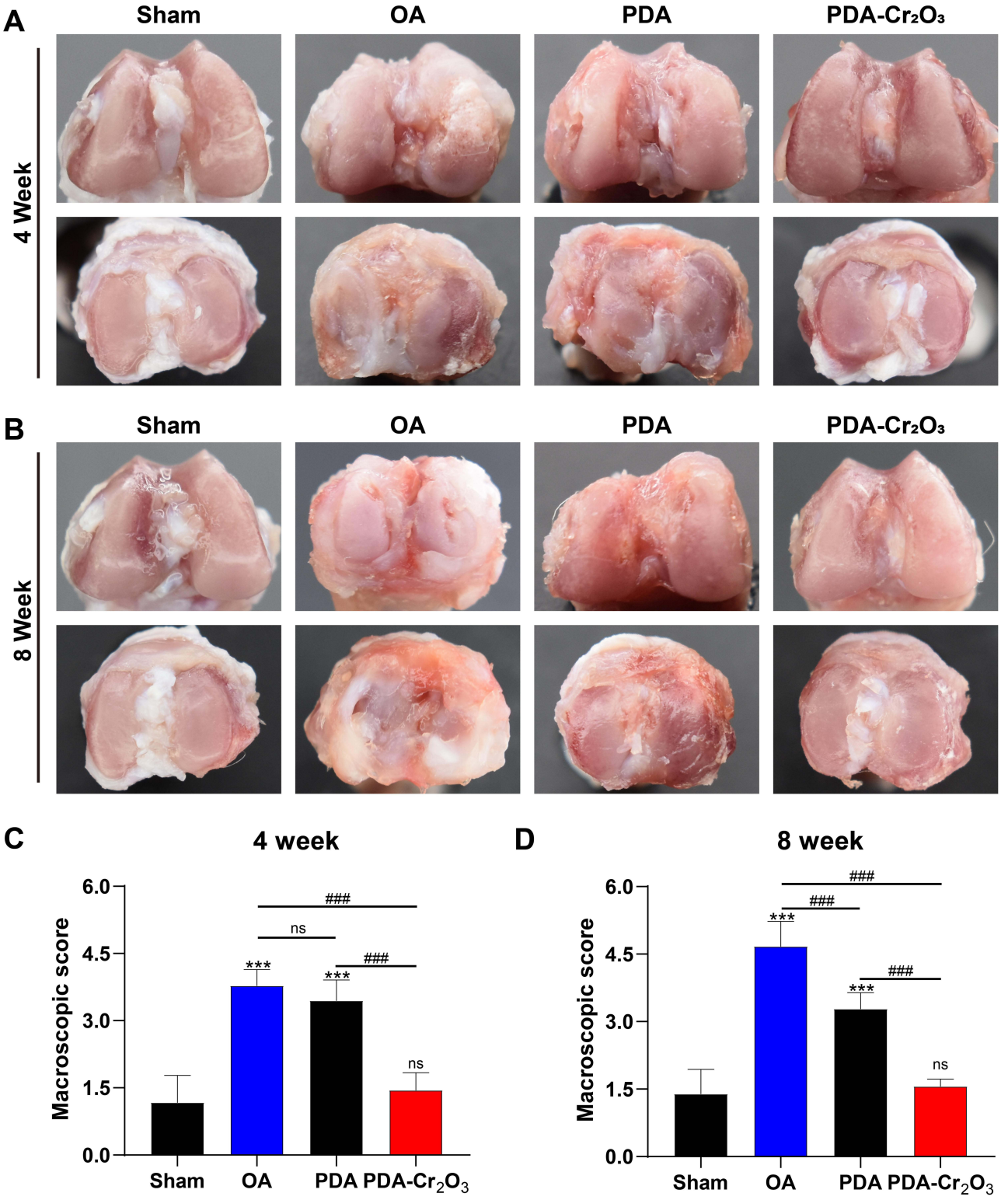

Figure 7 The gross images of the rat knee joints and the gross macroscopic scores. (**A**) Gross photographs of knee joints after a treatment duration of 4 weeks. (**B**) Gross photographs of knee joints after a treatment duration of 8 weeks. (**C**) Gross macroscopic scores of knee joints after a treatment duration of 4 weeks. (**D**) Gross macroscopic scores of knee joints after 8 weeks of treatment. The * symbol indicates comparisons between the sham group and all other groups, while the # symbol represents pairwise comparisons among the remaining groups. ***, ### indicates $p < 0.001$; ns indicates no significant.

https://doi.org/10.2147/IJN.S538289

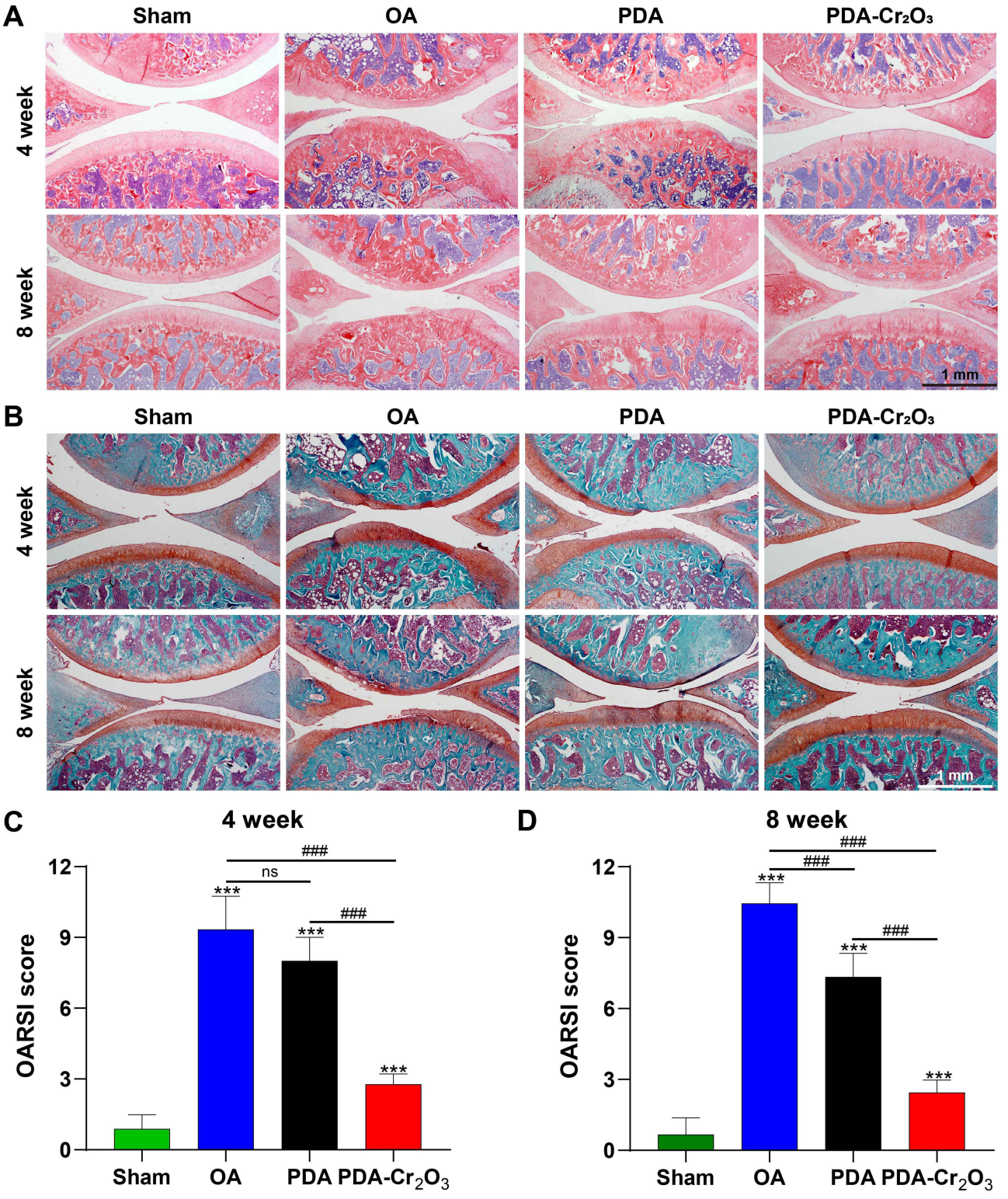

Figure 8 Histological results of rat knee joints. (**A**) HE staining pictures of knee joints. (**B**) Safranin-O staining pictures of knee joints. (**C**) OARSI scores of knee joints after a treatment duration of 4 weeks. (**D**) OARSI scores of knee joints after a treatment duration of 8 weeks. Scale bar: 1 mm. The * symbol indicates comparisons between the sham group and all other groups, while the # symbol represents pairwise comparisons among the remaining groups. ***, ### indicates $p < 0.001$; ns indicates no significant.

ROS scavenging agent because it is abundant in reducing chemical groups, such as catechols and imines, which release electrons to reduce ROS.[9,39,40] Several studies have been conducted to treat ROS-related diseases by scavenging ROS with PDA, and good results have been achieved.[9,41]

Reducing agents scavenge ROS through a direct redox reaction with ROS, and reducing agents will be progressively depleted with the process of scavenging ROS, so the effective treatment time is short, and repeated medication is required. Moreover, reducing agents are generally small molecules, which are quickly cleared from joints through the synovial vasculature. Consequently, high doses and high-frequency medication are required, and therefore side effects frequently occur.

Natural enzymes (including SOD and catalase) can reduce the level of intracellular ROS, which are essential to preserve the normal function of chondrocytes.[42] Gui et al used SOD-NPs to treat OA and achieved good efficacy.[43] However, natural enzymes suffer from the disadvantages of poor stability and harsh environmental requirements, which greatly limit their application.[39]

Since Lizeng Gao demonstrated that Fe_3O_4 nanomaterials have peroxidase-like activity in 2007, synthetic nanozymes have made rapid progress owing to the advantages of low cost, high stability, easy mass production, and storage.[10] Numerous studies have used synthetic nanozymes as ROS scavengers to treat OA. Kumar et al used polyethylene glycol-modified manganese dioxide to treat OA and found that the nanomaterial was able to efficiently remove H_2O_2. The material could remain in the joint for up to a week, providing a long-term therapeutic effect.[44] Although synthetic nanozymes have high enzyme activity, their application in the biomedical field is still limited because of high cytotoxicity, easy agglomeration, difficult degradation, and difficulty to enter cells.

In order to solve the above dilemma, we used the biocompatible material PDA to load synthetic nanozyme Cr_2O_3 and thus constructed a novel nanozyme PDA-Cr_2O_3. In our study, PDA-Cr_2O_3 showed good biocompatibility while retaining the efficient ability of scavenging ROS, and achieved good results to treat OA. Furthermore, compared to the work by Zhu et al, which used PDA nanoparticles to treat inflammatory depression, our PDA-Cr_2O_3 material showed a significantly superior ROS-scavenging capacity with a much lower dosage of 10 μg/kg, compared to the 10 mg/kg of PDA used in their study.[45] The sustained ROS-scavenging activity of PDA-Cr_2O_3, combined with its low dosage, offers an advantage in terms of reducing medication frequency and side effects, providing a more efficient therapeutic approach. In addition, compared to the study by Li et al on Mn_3O_4@PDA@Pd-SS31 nanozymes for OA treatment,[18] our PDA-Cr_2O_3 nanoparticles have a much simpler and cost-effective synthesis process. Li et al's approach involved a complex multi-step synthesis, whereas our material can be easily synthesized in two simple steps under room temperature conditions. This not only reduces production costs but also makes it more feasible for industrial scale-up and clinical translation.

This study provides a new idea for the treatment of ROS-related diseases such as OA, with a material that is simple to synthesize, highly effective, and more suitable for clinical application.

Conclusions

We first synthesized PDA-Cr_2O_3 nanozymes with homogeneous particle size distribution and good biocompatibility by simple methods. In vitro, PDA-Cr_2O_3 nanozymes are effective in scavenging various ROS, including H_2O_2 and $O_2^{\bullet-}$ and PDA-Cr_2O_3 nanozymes could effectively remove intracellular ROS, protect chondrocytes, and decrease the expression of inflammatory genes and the production of inflammatory proteins of OA chondrocytes. In vivo, PDA-Cr_2O_3 nanozymes achieved good therapeutic efficacy without significant toxic side effects. Our findings present a novel idea for the non-surgical treatment of OA. Future research should focus on evaluating the long-term therapeutic efficacy in chronic OA models and initiating preclinical investigations to facilitate the clinical translation of PDA-Cr_2O_3 nanozymes.

Funding

This research was financially supported by the Natural Science Foundation of Hubei Province (2024AFB1056), Open Research Fund of Obstetrics & Gynecology Institute, Xiangyang Central Hospital (2023MDI06), and Research Project of Xiangyang Central Hospital (2024YJ04B).

Disclosure

The authors declare no conflicts of interest in this work.

References

1. Li J, Zhang H, Han Y, Hu Y, Geng Z, Su J. Targeted and responsive biomaterials in osteoarthritis. *Theranostics*. 2023;13(3):931–954. doi:10.7150/thno.78639
2. Lin F, Wang Z, Xiang L, et al. Transporting hydrogel via chinese acupuncture needles for lesion positioning therapy. *Adv Sci*. 2022;9(17):e2200079. doi:10.1002/advs.202200079
3. Li Y, Tu Q, Xie D, et al. Triamcinolone acetonide-loaded nanoparticles encapsulated by CD90(+) MCSs-derived microvesicles drive anti-inflammatory properties and promote cartilage regeneration after osteoarthritis. *J Nanobiotechnol*. 2022;20(1):150. doi:10.1186/s12951-022-01367-z
4. Yao Q, Wu X, Tao C, et al. Osteoarthritis: pathogenic signaling pathways and therapeutic targets. *Signal Transduct Target Ther*. 2023;8(1):56. doi:10.1038/s41392-023-01330-w
5. Ansari MY, Ahmad N, Haqqi TM. Oxidative stress and inflammation in osteoarthritis pathogenesis: role of polyphenols. *Biomed Pharmacother*. 2020;129:110452. doi:10.1016/j.biopha.2020.110452
6. Yao H, Wang F, Chong H, et al. A curcumin-modified coordination polymers with ros scavenging and macrophage phenotype regulating properties for efficient ulcerative colitis treatment. *Adv Sci*. 2023;10(19):e2300601. doi:10.1002/advs.202300601
7. Xu J, Yu Y, Chen K, et al. Astragalus polysaccharides ameliorate osteoarthritis via inhibiting apoptosis by regulating ROS-mediated ASK1/p38 MAPK signaling pathway targeting on TXN. *Int J Biol Macromol*. 2024;258(Pt 2):129004. doi:10.1016/j.ijbiomac.2023.129004
8. Lee H, Dellatore SM, Miller WM, Messersmith PB. Mussel-inspired surface chemistry for multifunctional coatings. *Science*. 2007;318(5849):426–430. doi:10.1126/science.1147241
9. Bao X, Zhao J, Sun J, Hu M, Yang X. Polydopamine nanoparticles as efficient scavengers for reactive oxygen species in periodontal disease. *ACS Nano*. 2018;12(9):8882–8892. doi:10.1021/acsnano.8b04022
10. Gao L, Zhuang J, Nie L, et al. Intrinsic peroxidase-like activity of ferromagnetic nanoparticles. *Nat Nanotechnol*. 2007;2(9):577–583. doi:10.1038/nnano.2007.260
11. Khan SA, Shahid S, Hanif S, Almoallim HS, Alharbi SA, Sellami H. Green synthesis of chromium oxide nanoparticles for antibacterial, antioxidant anticancer, and biocompatibility activities. *Int J Mol Sci*. 2021;22(2):1.
12. Wang B, Xia X, Tang R, Jiang H, Qi M, Zhang X. Self-assembled Cr(2)O(3)@nanogel/Au nanozymes to simulate peroxidase activity as a H(2)O(2) sensor. *Spectrochim Acta A Mol Biomol Spectrosc*. 2023;285:121928. doi:10.1016/j.saa.2022.121928
13. Lu M, Cui Y, Zhao S, Fakhri A. Cr(2)O(3)/cellulose hybrid nanocomposites with unique properties: facile synthesis, photocatalytic, bactericidal and antioxidant application. *J Photochem Photobiol B Biol*. 2020;205:111842. doi:10.1016/j.jphotobiol.2020.111842
14. Marasini S, Tegafaw T, Miao X, et al. Relaxometric, optical and cell viability properties of D-glucuronic acid coated Cr_2O_3 nanoparticles. *J nanosci nanotechnol*. 2018;18(9):6333–6338. doi:10.1166/jnn.2018.15659
15. Chen C, Jian H, Mai K, et al. shape-and size-controlled synthesis of mn 3 o 4 nanocrystals at room temperature. *Eur J Inorg Chem*. 2014;2014(19). doi:10.1002/ejic.201400013
16. Guo H, Zheng R, Jiang H, Xu Z, Xia A. Preparation of sub-microspherical Fe(3)O(4)@PDA-Pd NPs catalyst and application in catalytic hydroreduction reaction of halogenated aromatic nitro compounds to prepare halogenated aromatic amines. *BMC Chem*. 2019;13(1):130. doi:10.1186/s13065-019-0649-9
17. Chang C, Liu H, Li X, et al. Combined ROS responsive polydopamine-coated berberine nanoparticles effective against ulcerative colitis in mouse model. *Int J Nanomed*. 2024;19:1205–1224. doi:10.2147/IJN.S442761
18. Li Y, Yang J, Chen X, et al. Mitochondrial-targeting and NIR-responsive Mn(3)O(4)@PDA@Pd-SS31 nanozymes reduce oxidative stress and reverse mitochondrial dysfunction to alleviate osteoarthritis. *Biomaterials*. 2024;305:122449. doi:10.1016/j.biomaterials.2023.122449
19. Huang H, Quan YY, Wang XP, Chen TS. Gold nanoparticles of diameter 13 nm induce apoptosis in rabbit articular chondrocytes. *Nanoscale Res Lett*. 2016;11(1):249. doi:10.1186/s11671-016-1461-2
20. Deng L, Ren R, Liu Z, et al. Stabilizing heterochromatin by DGCR8 alleviates senescence and osteoarthritis. *Nat Commun*. 2019;10(1):3329. doi:10.1038/s41467-019-10831-8
21. Pelletier JP, Fernandes JC, Brunet J, et al. In vivo selective inhibition of mitogen-activated protein kinase kinase 1/2 in rabbit experimental osteoarthritis is associated with a reduction in the development of structural changes. *Arthritis Rheum*. 2003;48(6):1582–1593. doi:10.1002/art.11014
22. Hao J, Ning Y, Hou Y, et al. Polydopamine functionalized graphene oxide membrane with the sandwich structure for osmotic energy conversion. *J Colloid Interface Sci*. 2023;630(Pt A):795–803. doi:10.1016/j.jcis.2022.10.084
23. Wang N, Gao Q, Tang J, et al. Anti-tumor effect of local injectable hydrogel-loaded endostatin alone and in combination with radiotherapy for lung cancer. *Drug Delivery*. 2021;28(1):183–194. doi:10.1080/10717544.2020.1869864
24. Chung MF, Chia WT, Wan WL, Lin YJ, Sung HW. Controlled release of an anti-inflammatory drug using an ultrasensitive ROS-responsive gas-generating carrier for localized inflammation inhibition. *J Am Chem Soc*. 2015;137(39):12462–12465. doi:10.1021/jacs.5b08057
25. He Y, Zhang Y, Zhang D, et al. 3-morpholinosydnonimine (SIN-1)-induced oxidative stress leads to necrosis in hypertrophic chondrocytes in vitro. *Biomed pharmacothe*. 2018;106:1696–1704. doi:10.1016/j.biopha.2018.07.128
26. Reed KN, Wilson G, Pearsall A, Grishko VI. The role of mitochondrial reactive oxygen species in cartilage matrix destruction. *Mol Cell Biochem*. 2014;397(1–2):195–201. doi:10.1007/s11010-014-2187-z
27. Bedingfield SK, Colazo JM, Yu F, et al. Amelioration of post-traumatic osteoarthritis via nanoparticle depots delivering small interfering RNA to damaged cartilage. *Nat Biomed Eng*. 2021;5(9):1069–1083. doi:10.1038/s41551-021-00780-3
28. Goldring MB, Birkhead JR, Suen LF, et al. Interleukin-1 beta-modulated gene expression in immortalized human chondrocytes. *J Clin Invest*. 1994;94(6):2307–2316. doi:10.1172/JCI117595
29. Ismail HM, Miotla-Zarebska J, Troeberg L, et al. Brief report: JNK-2 controls aggrecan degradation in murine articular cartilage and the development of experimental osteoarthritis. *Arthritis Rheumatol*. 2016;68(5):1165–1171. doi:10.1002/art.39547
30. Lee AS, Ellman MB, Yan D, et al. A current review of molecular mechanisms regarding osteoarthritis and pain. *Gene*. 2013;527(2):440–447. doi:10.1016/j.gene.2013.05.069

31. Lepetsos P, Papavassiliou KA, Papavassiliou AG. Redox and NF-κB signaling in osteoarthritis. *Free Radic Biol Med*. 2019;132:90–100. doi:10.1016/j.freeradbiomed.2018.09.025
32. Rathakrishnan C, Tiku K, Raghavan A, Tiku ML. Release of oxygen radicals by articular chondrocytes: a study of luminol-dependent chemiluminescence and hydrogen peroxide secretion. *J Bone Min Res*. 1992;7(10):1139–1148. doi:10.1002/jbmr.5650071005
33. Mendes AF, Caramona MM, Carvalho AP, Lopes MC. Hydrogen peroxide mediates interleukin-1beta-induced AP-1 activation in articular chondrocytes: implications for the regulation of iNOS expression. *Cell Biol Toxicol*. 2003;19(4):203–214. doi:10.1023/B:CBTO.0000003730.21261.fa
34. Marks PH, Donaldson ML. Inflammatory cytokine profiles associated with chondral damage in the anterior cruciate ligament-deficient knee. *Arthroscopy*. 2005;21(11):1342–1347. doi:10.1016/j.arthro.2005.08.034
35. Abramoff B, Caldera FE. Osteoarthritis: pathology, diagnosis, and treatment options. *Med Clin North Am*. 2020;104(2):293–311. doi:10.1016/j.mcna.2019.10.007
36. Di Francesco M, Fragassi A, Pannuzzo M, et al. Management of osteoarthritis: from drug molecules to nano/ micromedicines. *Wiley Interdiscip Rev Nanomed Nanobiotechnol*. 2022;14(3):e1780. doi:10.1002/wnan.1780
37. Shu C, Qin C, Chen L, et al. Metal-organic framework functionalized bioceramic scaffolds with antioxidative activity for enhanced osteochondral regeneration. *Adv Sci*. 2023;10(13):e2206875. doi:10.1002/advs.202206875
38. Liu Y, Ai K, Lu L. Polydopamine and its derivative materials: synthesis and promising applications in energy, environmental, and biomedical fields. *Chem Rev*. 2014;114(9):5057–5115. doi:10.1021/cr400407a
39. Guo X, Li Z, Liu S, et al. Studying the effect of PDA@CeO(2) nanoparticles with antioxidant activity on the mechanical properties of cells. *J Mat Chem B*. 2021;9(44):9204–9212. doi:10.1039/D1TB01918J
40. Zhao H, Zeng Z, Liu L, et al. Polydopamine nanoparticles for the treatment of acute inflammation-induced injury. *Nanoscale*. 2018;10(15):6981–6991. doi:10.1039/C8NR00838H
41. Lou X, Hu Y, Zhang H, Liu J, Zhao Y. Polydopamine nanoparticles attenuate retina ganglion cell degeneration and restore visual function after optic nerve injury. *J Nanobiotechnol*. 2021;19(1):436. doi:10.1186/s12951-021-01199-3
42. Afonso V, Champy R, Mitrovic D, Collin P, Lomri A. Reactive oxygen species and superoxide dismutases: role in joint diseases. *Joint Bone Spine*. 2007;74(4):324–329. doi:10.1016/j.jbspin.2007.02.002
43. Gui T, Luo L, Chhay B, et al. Superoxide dismutase-loaded porous polymersomes as highly efficient antioxidant nanoparticles targeting synovium for osteoarthritis therapy. *Biomaterials*. 2022;283:121437. doi:10.1016/j.biomaterials.2022.121437
44. Kumar S, Adjei IM, Brown SB, Liseth O, Sharma B. Manganese dioxide nanoparticles protect cartilage from inflammation-induced oxidative stress. *Biomaterials*. 2019;224:119467. doi:10.1016/j.biomaterials.2019.119467
45. Zhu T-T, Wang H, Gu H-W, et al. Melanin-like polydopamine nanoparticles mediating anti-inflammatory and rescuing synaptic loss for inflammatory depression therapy. *J Nanobiotechnol*. 2023;21(1):52. doi:10.1186/s12951-023-01807-4